6.977 Ultrafast Optics

Franz X. Kaertner

Spring Term 2005

Contents

Chapter 1

Introduction

1.1 Course Mission

- Generation of ultrashort pulses: Nano-, Pico-, Femto-, Attosecond Pulses
- Propagation of ultrashort pulses
- Linear and nonlinear effects.
- Applications in high precision measurements, nonlinear optics, optical signal processing, optical communications, x-ray generation,....

1.2 Pulse Characteristics

Most often, there is not an isolated pulse, but rather a pulse train.

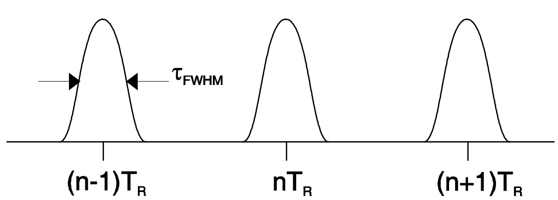

Figure 1.1: Periodic pulse train

T_R: pulse repetition time
W : pulse energy
$P_{ave} = W/T_R$: average power
τ_{FWHM} is the Full Width at Half Maximum of the intensity envelope of the pulse in the time domain.
The peak power is given by

$$P_p = \frac{W}{\tau_{\mathrm{FWHM}}} = P_{ave}\,\frac{T_R}{\tau_{\mathrm{FWHM}}}, \tag{1.1}$$

and the peak electric field is given by

$$E_p = \sqrt{2Z_{F_0}\frac{P_p}{A_{\mathrm{eff}}}}. \tag{1.2}$$

A_{eff} is the beam cross-section and $Z_{F_0} = 377\,\Omega$ is the free space impedance.

<u>Time scales</u>:

1 ns	$\sim$	30 cm	(high-speed electronics, GHz)
1 ps	$\sim$	300 μm	
1 fs	$\sim$	300 nm	
1 as $= 10^{-18}$ s	$\sim$	0.3 nm $= 3$ Å	(typ-lattice constant in metal)

The shortest pulses generated to date are about $4-5$ fs at 800 nm ($\lambda/c = 2.7$ fs), less than two optical cycles and 250 as at 25 nm. For few-cycle pulses, the electric field becomes important, not only the intensity!

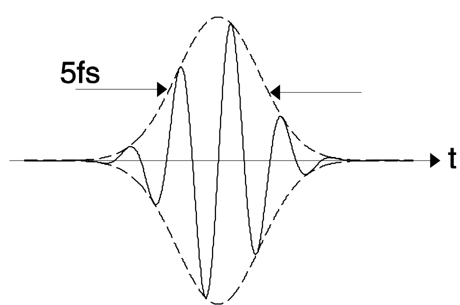

Figure 1.2: Electric field waveform of a 5 fs pulse at a center wavelength of 800 nm. The electric field depends on the carrier-envelope phase.

average power:

$$P_{ave} \sim \begin{array}{l} 1W, \text{ up to 100 W in progress.} \\ kW \text{ possible, not yet pulsed} \end{array}$$

repetition rates:

$$T_R^{-1} = f_R = \mathrm{mHz} - 100\,\mathrm{GHz}$$

pulse energy:

$$W = 1\mathrm{pJ} - 1\mathrm{kJ}$$

pulse width:

$$\tau_{\mathrm{FWHM}} = \begin{array}{cc} 5\,\mathrm{fs} - 50\,\mathrm{ps}, & \text{modelocked} \\ 30\,\mathrm{ps} - 100\,\mathrm{ns}, & \mathrm{Q-switched} \end{array}$$

peak power:

$$P_p = \frac{1\,\mathrm{kJ}}{1\,\mathrm{ps}} \sim 1\,\mathrm{PW},$$

obtained with Nd:glass (LLNL - USA, [1][2][3]).

For a typical lab pulse, the peak power is

$$P_p = \frac{10\,\mathrm{nJ}}{10\,\mathrm{fs}} \sim 1\,\mathrm{MW}$$

peak field of typical lab pulse:

$$E_p = \sqrt{2 \times 377 \times \frac{10^6 \times 10^{12}}{\pi \times (1.5)^2}\frac{\mathrm{V}}{\mathrm{m}}} \approx 10^{10}\frac{\mathrm{V}}{\mathrm{m}} = \frac{10\,\mathrm{V}}{\mathrm{nm}}$$

1.3 Applications

- High time resolution: Ultrafast Spectroscopy, tracing of ultrafast physical processes in condensed matter (see Fig. 1.3), chemical reactions, physical and biological processes, influence chemical reactions with femtosecond pulses: Femto-Chemistry (Noble Prize, 2000 to A. Zewail), high speed electric circuit testing and sampling of electrical signals, see Fig. 1.4.

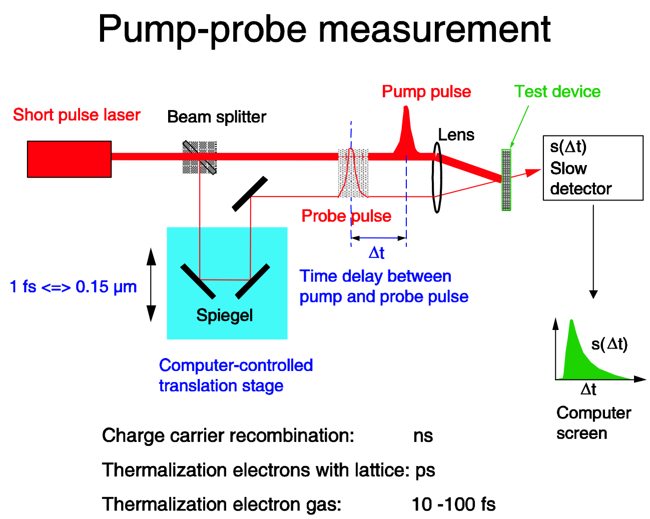

Figure 1.3: Pump-probe setup to extract time constants relevant for the carrier dynamics in semiconductors.

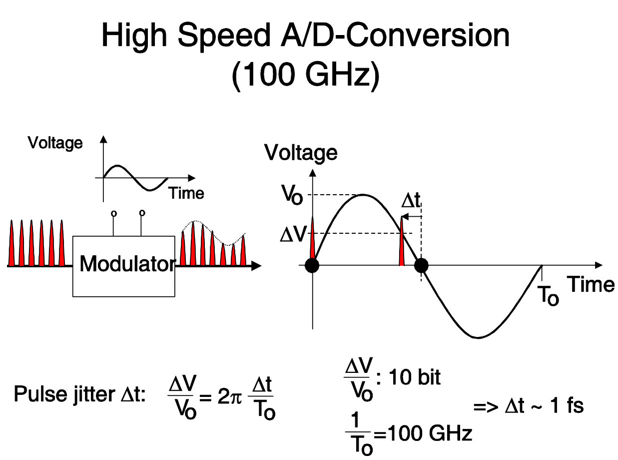

Figure 1.4: High speed A/D conversion with a high repetition rate pico- or femtosecond laser.

- High spatial resolution: $c\tau_{\mathrm{FWHM}}$; optical imaging, e.g. optical coherence tomography, see Figs. 1.5-1.8).

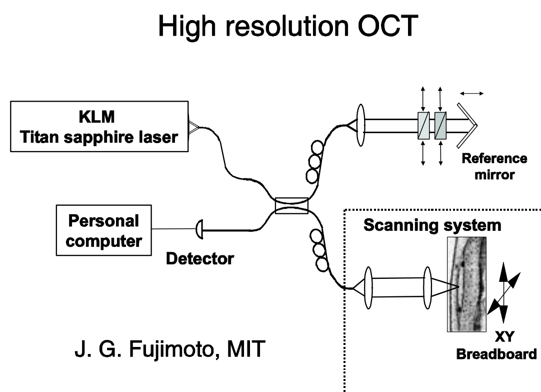

Figure 1.5: Setup for optical coherence tomography.

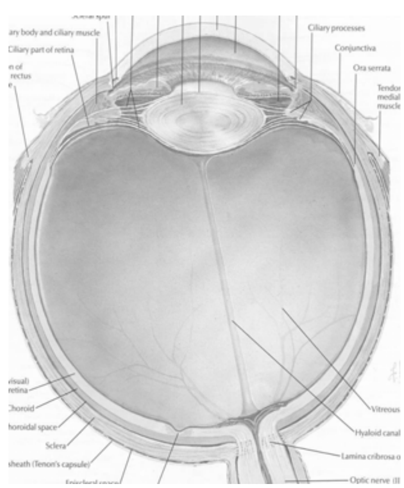

Figure 1.6: Cross section through the human eye.

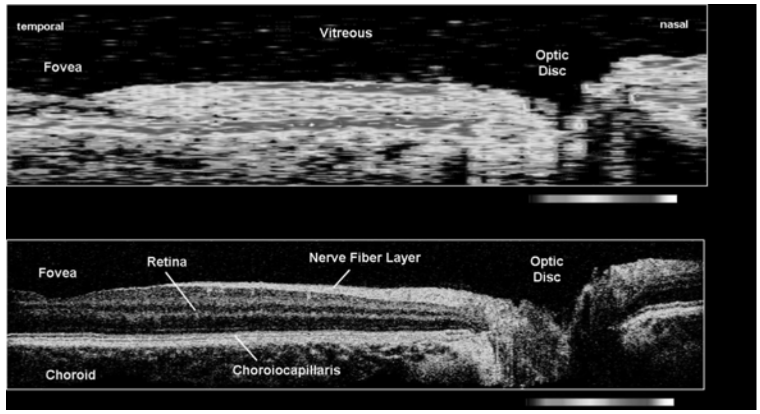

Figure 1.7: Comparison of retinal images taken with a superluminescence diode (top) versus a broadband Ti:sapphire laser (below).

- Imagaing through strongly scattering media:

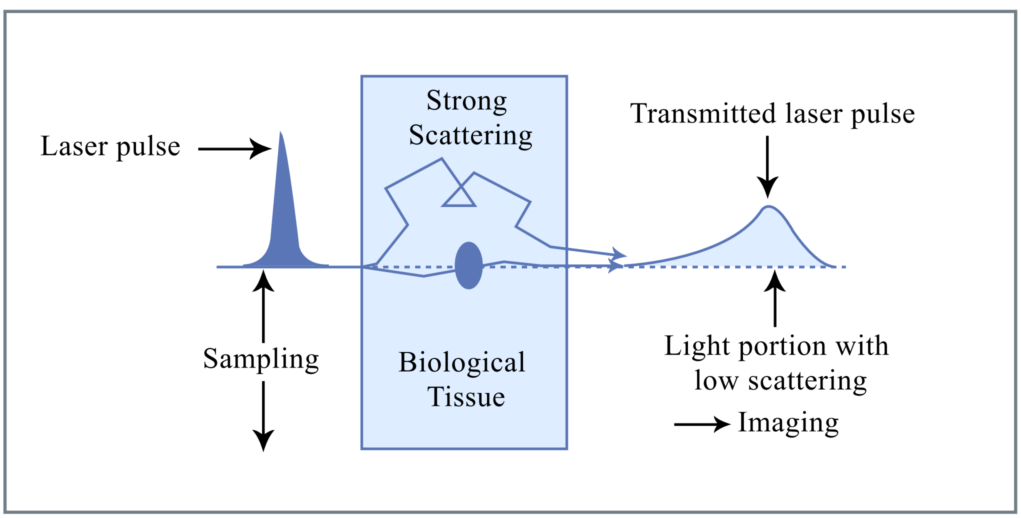

Figure 1.8: Imaging of the directly transmitted photons results in an unblurred picture. Substitution for x-ray imaging; however, transmission is very low.

- High bandwidth: massive WDM - optical communications, many channels from one source or massive TDM, high bit-rate stream of short pulses.

- High intensities: Large intensities at low average power $\Rightarrow$ Nonlinear frequency conversion, laser material processing, surgery, high intensity physics: x-ray generation, particle acceleration, ...

1.4 Review of Laser Essentials

Linear and ring cavities:

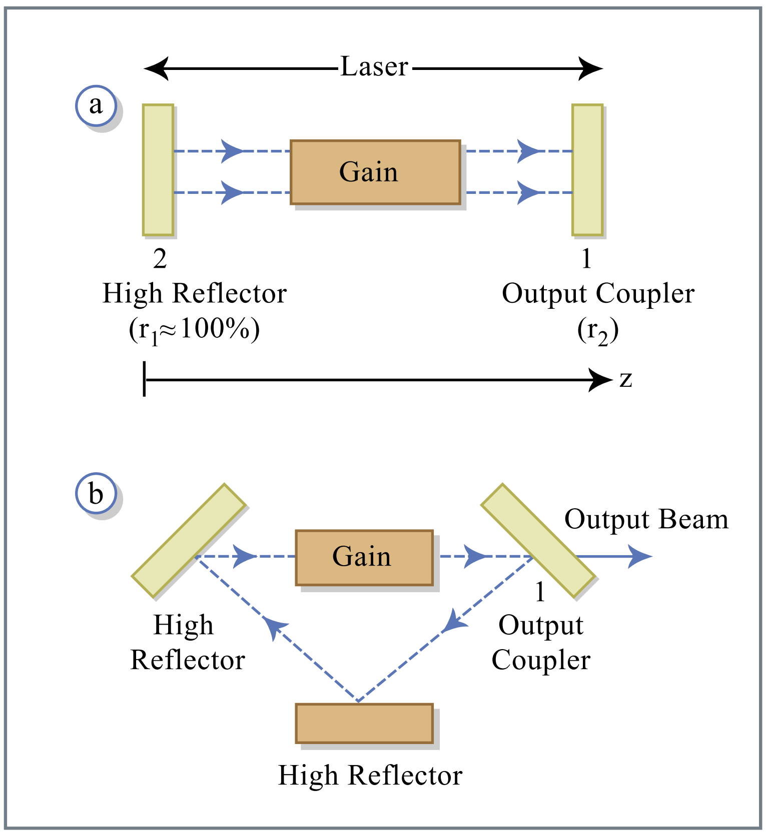

Figure 1.9: Possible cavity configurations. (a) Schematic of a linear cavity laser. (b) Schematic of a ring laser. [1]

Steady-state operation: Electric field must repeat itself after one roundtrip. Consider a monochromatic, linearly polarized field

$$E(z,t) = \Re\left\{E_0 e^{\mathrm{j}(\omega t - kz)}\right\}, \tag{1.3}$$

where

$$k = \frac{\omega}{c} n \tag{1.4}$$

is the propagation constant in a medium with refractive index n.

Consider linear resonator in Fig. 1.9a. Propagation from (1) to (2) is determined by $n = n' + \mathrm{j}n''$ (complex refractive index), with the electric field given by

$$E = \Re\left\{ E_0 e^{\frac{\omega}{c} n_g'' \ell_g} e^{\mathrm{j}\omega t} e^{-\mathrm{j}\frac{\omega}{c}(n_g' \ell_g + \ell_a)} \right\}, \tag{1.5}$$

where n_g is the complex refractive index of the gain medium (outside the gain medium $n = 1$ is assumed), ℓ_g is the length of the gain medium, ℓ_a is the outside gain medium, and $\ell = n_g \ell_g + \ell_a$ is the optical path length in the resonator.

Propagation back to (1), i.e. one full roundtrip results in

$$E = \Re\left\{ r_1 r_2 e^{2\frac{\omega}{c} n_g'' \ell_g} E_0 e^{\mathrm{j}\omega t - \mathrm{j}2\frac{\omega}{c}\ell} \right\} \Rightarrow r_1 r_2 e^{2\frac{\omega}{c} n_g'' \ell_g} = 1, \tag{1.6}$$

i.e. the gain equals the loss, and furthermore, we obtain the phase condition

$$\frac{2\omega\ell}{c} = 2m\pi. \tag{1.7}$$

The phase condition determines the resonance frequencies, i.e.

$$\omega_m = \frac{m\pi c}{\ell} \tag{1.8}$$

and

$$f_m = \frac{mc}{2\ell}. \tag{1.9}$$

The mode spacing of the longitudinal modes is

$$\Delta f = f_m - f_{m-1} = \frac{c}{2\ell} \tag{1.10}$$

(only true if there is no dispersion, i.e. $n \neq n(\omega)$). Assume frequency independent cavity loss and bell shaped gain (see Fig. 1.10).

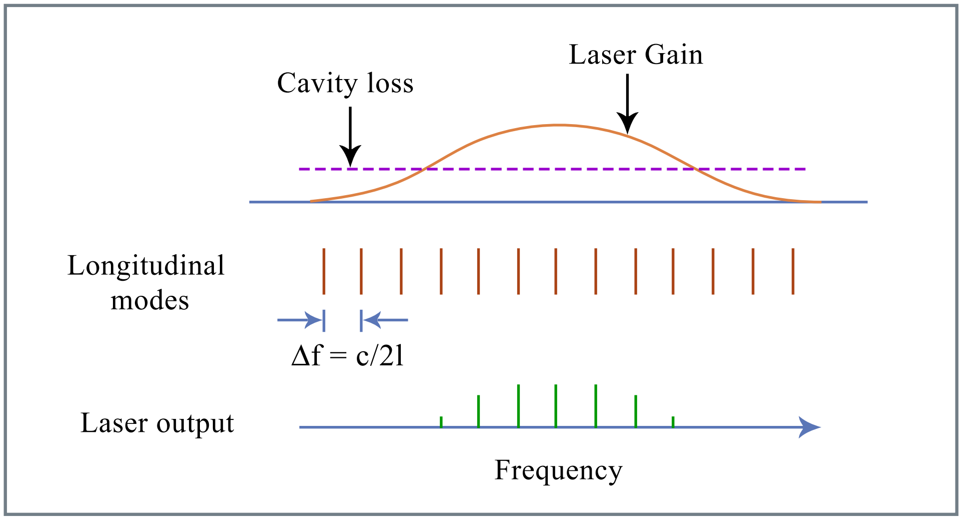

Figure 1.10: Laser gain and cavity loss spectra, longitudinal mode location, and laser output for multimode laser operation.

Figure by MIT OCW.

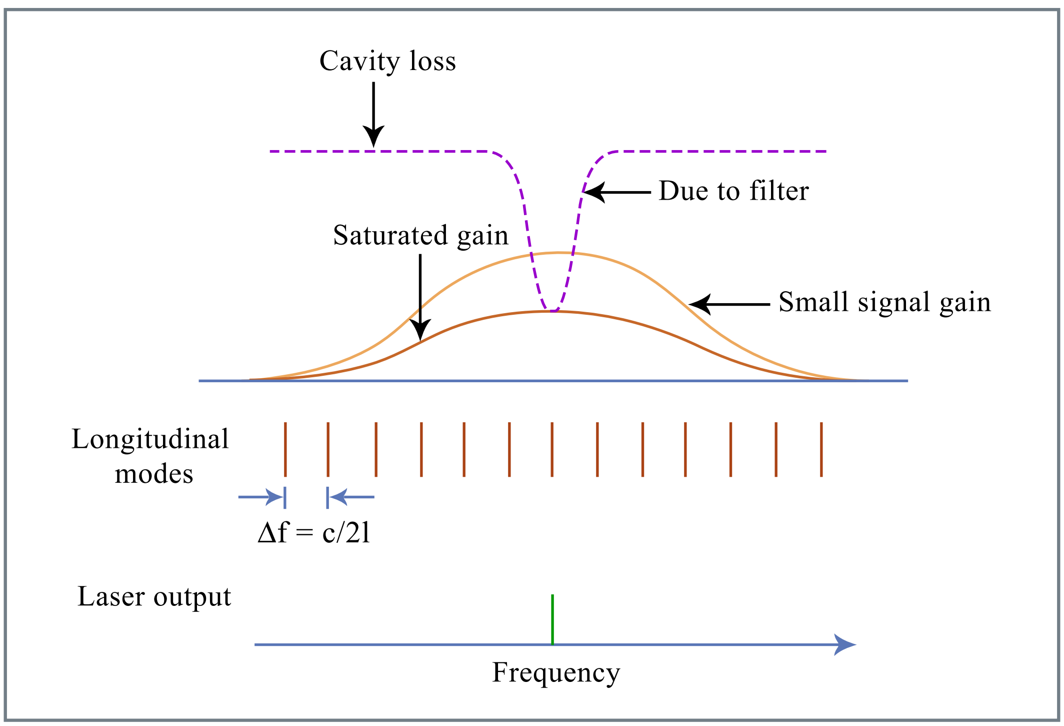

Figure 1.11: Gain and loss spectra, longitudinal mode locations, and laser output for single mode laser operation.

Figure by MIT OCW.

To assure single frequency operation use filter (etalon); distinguish between homogeneously and inhomogeneously broadened gain media, effects of spectral hole burning! Distinguish between small signal gain g_0 per roundtrip, i.e. gain for laser intensity $I \rightarrow 0$, and large signal gain, most often given by

$$g = \frac{g_0}{1 + \frac{I}{I_{\text{sat}}}}, \tag{1.11}$$

where I_{sat} is the saturation intensity. Gain saturation is responsible for the steady state gain (see Fig. 1.11), and homogeneously broadened gain is assumed.

To generate short pulses, i.e. shorter than the cavity roundtrip time, we wish to have many longitudinal modes runing in steady state. For a multimode laser the laser field is given by

$$E(z,t) = \Re\left[\sum_m \hat{E}_m e^{\mathrm{j}(\omega_m t - k_m z + \phi_m)}\right], \tag{1.12a}$$

$$\omega_m = \omega_0 + m\Delta\omega = \omega_0 + \frac{m\pi c}{\ell}, \tag{1.12b}$$

$$k_m = \frac{\omega_m}{c}, \tag{1.12c}$$

where the symbol ˆ denotesa frequency domain quantity. Equation (1.12a) can be rewritten as

$$E(z,t) = \Re\left\{e^{\mathrm{j}\omega_0(t-z/c)} \sum_m \hat{E}_m e^{\mathrm{j}(m\Delta\omega(t-z/c)+\phi_m)}\right\} \tag{1.13a}$$

$$= \Re\left[A(t-z/c)e^{\mathrm{j}\omega_0(t-z/c)}\right] \tag{1.13b}$$

with the complex envelope

$$A\left(t - \frac{z}{c}\right) = \sum_m E_m e^{\mathrm{j}(m\Delta\omega(t-z/c)+\phi_m)} = \text{complex envelope (slowly varying)}. \tag{1.14}$$

$e^{\mathrm{j}\omega_0(t-z/c)}$ is the carrier wave (fast oscillation). Both carrier and envelope travel with the same speed (no dispersion assumed). The envelope function is periodic with period

$$T = \frac{2\pi}{\Delta\omega} = \frac{2\ell}{c} = \frac{L}{c}. \tag{1.15}$$

L is the roundtrip length (optical)!

<u>Examples:</u>

Examples:

We assume N modes with equal amplitudes $E_m = E_0$ and equal phases $\phi_m = 0$, and thus the envelope is given by

$$A(z,t) = E_0 \sum_{m=-(N-1)/2}^{(N-1)/2} e^{\mathrm{j}(m\Delta\omega(t-z/c))}. \tag{1.16}$$

With

$$\sum_{m=0}^{q-1} a^m = \frac{1-a^q}{1-a}, \tag{1.17}$$

we obtain

$$A(z,t) = E_0 \frac{\sin\left[\frac{N\Delta\omega}{2}\left(t-\frac{z}{c}\right)\right]}{\sin\left[\frac{\Delta\omega}{2}\left(t-\frac{z}{c}\right)\right]}. \tag{1.18}$$

The laser intensity I is proportional to $E(z,t)^2$, averaged over one optical cycle: $I \sim |A(z,t)|^2$. At $z=0$, we obtain

$$I(t) \sim |E_0|^2 \frac{\sin^2\left(\frac{N\Delta\omega t}{2}\right)}{\sin^2\left(\frac{\Delta\omega t}{2}\right)}. \tag{1.19}$$

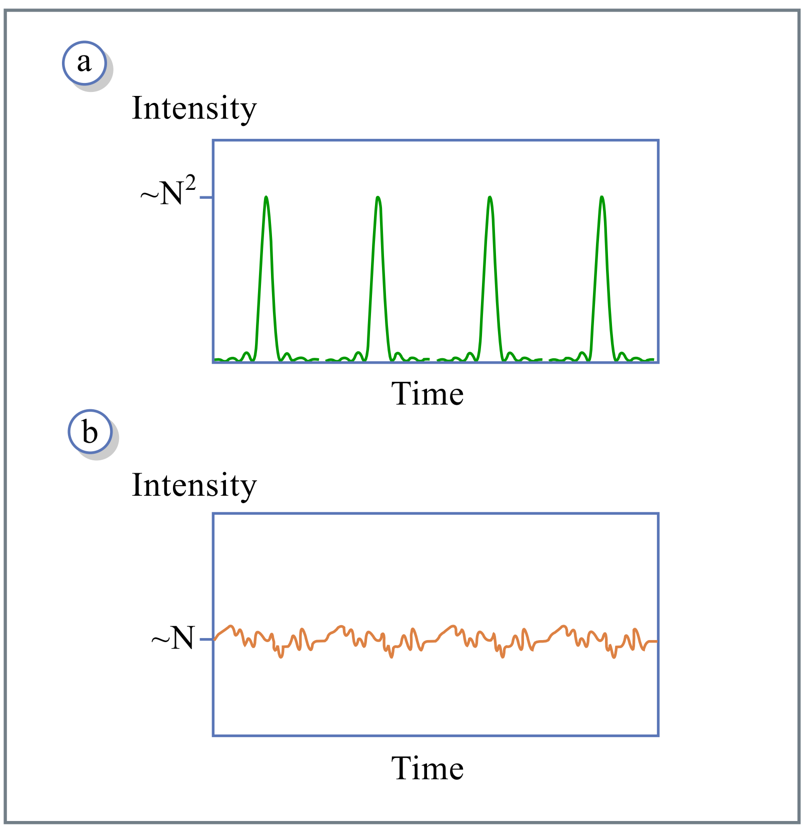

Figure 1.12: (a) mode-locked laser output with constant mode phase. (b) Laser output with randomly phased modes.

Figure by MIT OCW.

(a) Periodic pulses given by Eq. (1.19), period $T = 1/\Delta f = L/c$

- pulse duration
$$\Delta t = \frac{2\pi}{N\Delta\omega} = \frac{1}{N\Delta f} \tag{1.20}$$
- peak intensity $\sim N^2|E_0|^2$
- average intensity $\sim N|E_0|^2 \Rightarrow$ peak intensity is enhanced by a factor N.

(b) If phases of modes are not locked, i.e. ϕ_m random sequence

- Intensity fluctuates randomly about average value ($\sim N|E_0|^2$), same as modelocked case
- correlation time is $\Delta t_c \approx \frac{1}{N \cdot \Delta f}$
- Fluctuations are still periodic with period $T = 1/\Delta f$.

In a usual multimode laser, ϕ_m varies over t.

1.5 History

1960: First laser, ruby, Maiman [4].

1961: Proposal for Q-switching, Hellwarth [5].

1963: First indications of mode locking in ruby lasers, Guers and Mueller [6],[7], Statz and Tang [8]. on He-Ne lasers.

1964: Activemodelocking (HeNe, Ar, etc.), DiDomenico [9], [10] and Yariv [11].

1966: Passive modelocking with saturable dye absorber in ruby by A. J. Dellaria, Mocker and Collins [12].

1966: Dye laser, F. P. Schäfer, et al. [13].

1968: mode-locking (Q-Switching) of dye-lasers, Schmidt, Schäfer [14].

1972: cw-passive modelocking of dye laser, Ippen, Shank, Dienes [15].

1972: Analytic theories on active modelocking [21, 22].

1974: Sub-ps-pulses, Shank, Ippen [16].

1975: Theories for passive modelocking with slow [1], [24] and fast saturable absorbers [25] predicted hyperbolic secant pulse.

1981: Colliding-pulse mode-locked laser (CPM), [17].

1982: Pulse compression [20].

1984: Soliton Laser, Mollenauer, [26].

1985: Chirped pulse amplification, Strickland and Morou, [27].

1986: Ti:sapphire (solid-state laser), P. F. Moulton [28].

1987: 6 fs at 600 nm, external compression, Fork et al. [18, 19].

1988: Additive Pulse Modelocking (APM),[29, 30, 31].

1991: Kerr-lens modelocking, Spence et al. [32, 33, 34, 35, 36].

1993: Streched pulse laser, Tamura et al [37].

1994: Chirped mirrors, Szipoecs et al. [38, 39]

1997: Double-chirped mirrors, Kaertner et al.[40]

2001: 5 fs, sub-two cycle pulses, octave spanning, Ell at. al.[42]

2001: 250 as by High-Harmonic Generation, Krausz et al.[43]

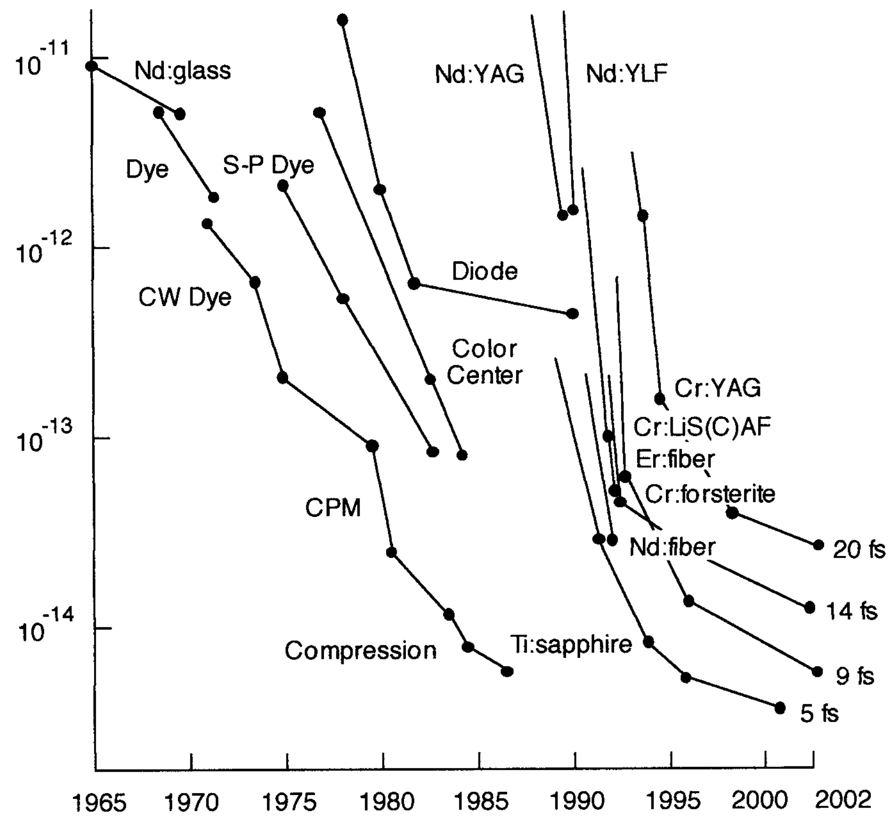

Figure 1.13: Pulse width of different laser systems by year.

Courtesy of Erich Ippen. Used with permission.

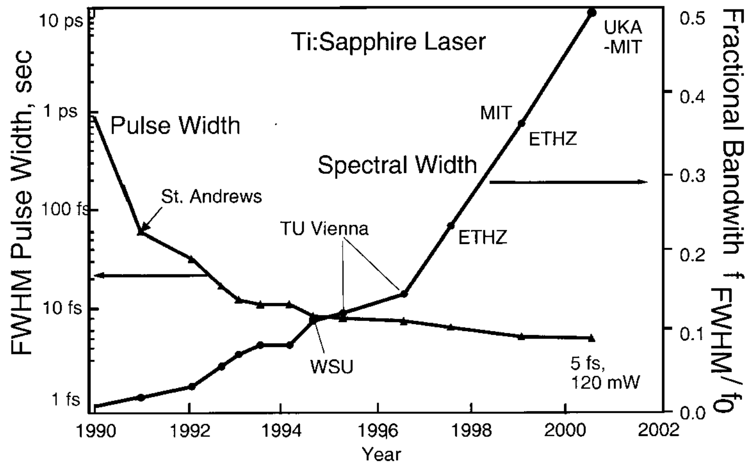

Figure 1.14: Pulse width of Ti:sapphire lasers by year.

1.6 Laser Materials

Laser Material	Absorption Wavelength	Average Emission λ	Band Width	Pulse Width
Nd:YAG	808 nm	1064 nm	0.45 nm	$\sim$ 6 ps
Nd:YLF	797 nm	1047 nm	1.3 nm	$\sim$ 3 ps
Nd:LSB	808 nm	1062 nm	4 nm	$\sim$ 1.6 ps
Nd:YVO_4	808 nm	1064 nm	2 nm	$\sim$ 4.6 ps
Nd:fiber	804 nm	1053 nm	22-28 nm	$\sim$ 33 fs
Nd:glass	804 nm	1053 nm	22-28 nm	$\sim$ 60 fs
Yb:YAG	940, 968 nm	1030 nm	6 nm	$\sim$ 300 fs
Yb:glass	975 nm	1030 nm	30 nm	$\sim$ 90 fs
Ti:Al_2O_3	480-540 nm	796 nm	200 nm	$\sim$ 5 fs
Cr^{4+}:Mg_2SiO_4:	900-1100 nm	1260 nm	200 nm	$\sim$ 14 fs
Cr^{4+}:YAG	900-1100 nm	1430 nm	180 nm	$\sim$ 19 fs

Transition metals: (Cr^{3+}, Ti^{3+}, Ni^{2+}, CO^{2+}, etc.) (outer $3d$-electrons) $\rightarrow$ broadband

Rare earth: (Nd^{3+}, Tm^{3+}, Ho^{3+}, Er^{3+}, etc.) (shielded $4f$-electrons) $\rightarrow$ narrow band.

Bibliography

[1] M. D. Perry and G. Mourou, "Terawatt to Petawatt Subpicosecond Lasers," Science, Vol. 264 (1994), p. 917.

[2] M. D. Perry et al., "Petawatt Laser Pulses," Optics Letters, Vol. 24 (1999), p. 160.

[3] T. Tajima and G. Mourou, Phys. Rev. Spec. Topics-Accelerators and Beams 5(031301) 1 (2002). See also wwwapr.apr.jaeri.go.jp/aprc/e/index_e.html, www.eecs.umich.edu/CUOS/HERCULES/index, www.clf.rl.ac.uk

[4] T. H. Maimann, "Stimulated optical radiation in ruby", Nature **187**, 493-494, (1960).

[5] R. W. Hellwarth, Ed., *Advances in Quantum Electronics*, Columbia Press, NY (1961).

[6] K. Gürs, R. Müller: "Breitband-modulation durch Steuerung der emission eines optischen masers (Auskoppel-modulation)", Phys. Lett. **5**, 179-181 (1963).

[7] K. Gürs (Ed.): "Beats and modulation in optical ruby laser," in *Quantum Electronics III* (Columbia University Press, New York 1964).

[8] H. Statez, C.L. Tang (Eds.): "Zeeman effect and nonlinear interactions between oscillationg laser modes", in *Quantum Electronics III* (Columbia University Press, New York 1964).

[9] M. DiDomenico: "Small-signal analysis of internal (coupling type) modulation of lasers," J. Appl. Phys. **35**, 2870-2876 (1964).

[10] L.E. Hargrove, R.L. Fork, M.A. Pollack: "Locking of He-Ne laser modes induced by synchronous intracavity modulation," Appl. Phys. Lett. **5**, 4-5 (1964).

[11] A. Yariv: "Internal modulation in multimode laser oscillators," J. Appl. Phys. **36**, 388-391 (1965).

[12] H.W. Mocker, R.J. Collins: "Mode competition and self-locking effects in a Q-switched ruby laser," Appl. Phys. Lett. **7**, 270-273 (1965).

[13] F. P. Schäfer, F. P. W. Schmidt, J. Volze: "Organic Dye Solution Laser," Appl. Phys. Lett. $\mathbf{9}, 306-308$ (1966).

[14] F. P. W. Schmidt, F. P. Schäfer: "Self-mode-locking of dye-lasers with saturable absorbers," Phys. Lett. 26A, 258-259 (1968).

[15] E.P. Ippen, C.V. Shank, A. Dienes: "Passive mode locking of the cw dye laser," Appl. Phys. Lett. **21**, 348-350 (1972)·

[16] C.V. Shank, E.P. Ippen: "Sub-picosecond kilowatt pulses from a mode-locked cw dye laser," Appl. Phys. Lett. **24**, 373-375 (1974).

[17] R.L. Fork, B.I. Greene, C.V. Shank: "Generation of optical pulses shorter than 0.1 psec by colliding pulse mode-locking," Appl. Phys. Lett. **38**, 617-619 (1981).

[18] W.H. Knox, R.L. Fork, M.C. Downer, R.H. Stolen, C.V. Shank, J.A. Valdmanis: "Optical pulse compression to 8 fs at a 5-kHz repetition rate," Appl. Phys. Lett. **46**, 1120-1122 (1985).

[19] R.L. Fork, C.H.B. Cruz, P.C. Becker, C.V. Shank: "Compression of optical pulses to six femtoseconds by using cubic phase compensation," Opt. Lett. **12**, 483-485 (1987).

[20] D. Grischowsky, A. C. Balant: TITLE, Appl. Phys. Lett. **41**, pp. (1982).

[21] J. Kuizenga, A. E. Siegman: "FM und AM mode locking of the homogeneous laser - Part I: Theory, IEEE J. Quantum Electron. **6**, 694-708 (1970).

[22] J. Kuizenga, A. E. Siegman: "FM und AM mode locking of the homogeneous laser - Part II: Experimental results, IEEE J. Quantum Electron. **6**, 709-715 (1970).

[23] G.H.C. New: Pulse evolution in mode-locked quasicontinuous lasers, IEEE J. Quantum Electron. **10**, 115-124 (1974).

[24] H.A. Haus: Theory of mode locking with a slow saturable absorber, IEEE J. Quantum Electron. **QE 11**, 736-746 (1975).

[25] H.A. Haus, C.V. Shank, E.P. Ippen: Shape of passively mode-locked laser pulses, Opt. Commun. **15**, 29-31 (1975).

[26] L.F. Mollenauer, R.H. Stolen: The soliton laser, Opt. Lett. **9**, 13-15 (1984).

[27] D. Strickland and G. Morou: "Chirped pulse amplification," Opt. Comm. **56**,229-221,(1985).

[28] P. F. Moulton: "Spectroscopic and laser characteristics of Ti:Al2O3", JOSA B **3**, 125-132 (1986).

[29] K. J. Blow and D. Wood: "Modelocked Lasers with nonlinear external cavity," J. Opt. Soc. Am. B 5, 629-632 (1988).

[30] J. Mark, L.Y. Liu, K.L. Hall, H.A. Haus, E.P. Ippen: Femtosecond pulse generation in a laser with a nonlinear external resonator, Opt. Lett. **14**, 48-50 (1989)·

[31] E.P. Ippen, H.A. Haus, L.Y. Liu: Additive pulse modelocking, J. Opt. Soc. Am. B **6**, 1736-1745 (1989).

[32] D.E. Spence, P.N. Kean, W. Sibbett: 60-fsec pulse generation from a self-mode-locked Ti:Sapphire laser, Opt. Lett. **16**, 42-44 (1991).

[33] D.K. Negus, L. Spinelli, N. Goldblatt, G. Feugnet: TITLE, in *Advanced Solid-State Lasers* G. Dubé, L. Chase (Eds.) (Optical Society of America, Washington, D.C., 1991) pp. 120-124.

[34] F. Salin, J. Squier, M. Piché: Mode locking of Ti:Al_2O_3 lasers and self-focusing: A Gaussian approximation, Opt. Lett. **16**, 1674-1676 (1991).

[35] M. Piché: Beam reshaping and self-mode-locking in nonlinear laser resonators, Opt. Commun. **86**, 156-160 (1991)

[36] U. Keller, G.W. 'tHooft, W.H. Knox, J.E. Cunningham: TITLE, Opt. Lett. **16**, 1022-1024 (1991).

[37] K. Tamura, E.P. Ippen, H.A. Haus, L.E. Nelson: 77-fs pulse generation from a stretched-pulse mode-locked all-fiber ring laser, Opt. Lett. **18**, 1080-1082 (1993)

[38] A. Stingl, C. Spielmann, F. Krausz: "Generation of 11-fs pulses from a Ti:sapphire laser without the use of prism," Opt. Lett. **19**, 204-206 (1994)

[39] R. Szipöcs, K. Ferencz, C. Spielmann, F. Krausz: Chirped multilayer coatings for broadband dispersion control in femtosecond lasers, Opt. Lett. **19**, 201-203 (1994)

[40] F.X. Kärtner, N. Matuschek, T. Schibli, U. Keller, H.A. Haus, C. Heine, R. Morf, V. Scheuer, M. Tilsch, T. Tschudi: Design and fabrication of double-chirped mirrors, Opt. Lett. **22**, 831-833 (1997)

[41] Y. Chen, F.X. Kärtner, U. Morgner, S.H. Cho, H.A. Haus, J.G. Fujimoto, E.P. Ippen: Dispersion-managed mode locking, J. Opt. Soc. Am. B **16**, 1999-2004 (1999)

[42] R. Ell, U. Morgner, F.X. Kärtner, J.G. Fujimoto, E.P. Ippen, V. Scheuer, G. Angelow, T. Tschudi: Generation of 5-fs pulses and octave-spanning spectra directly from a Ti:Sappire laser, Opt. Lett. **26**, 373-375 (2001)

[43] H. Hentschel, R. Kienberger, Ch. Spielmann, G. A. Reider, N. Milosevic, T. Brabec, P. Corkum, U. Heinzmann, M. Drescher, F. Krausz: "Attosecond Metrology," Nature **414**, 509-513 (2001).